Convective Mass Transfer From Submerged Superhydrophobic Surfaces: Turbulent Flow

Christina A. Barth[1], Mohamed A. Samaha[2], Hooman Vahedi Tafreshi[1] and Mohamed Gad-el-Hak[1]
[1]Department of Mechanical & Nuclear Engineering, Virginia Commonwealth University, Richmond, VA 23284
[2]Department of Mechanical & Aerospace Engineering, Princeton University, Princeton, NJ 08544

Received date 31/7/2013; Accepted date 7/9/2013

ABSTRACT
Superhydrophobic surfaces have received considerable attention in recent years. The surface has a strong water-repellent characteristic that could produce slip flow and drag reduction. The coating traps air within its micropores, such that a submerged moving body experiences shear-free and no-slip regions over, respectively, the air pockets and the solid surface. This, in turn, holds promise for a broad range of applications. Longevity of the entrapped air is an outstanding problem for these coatings. Under pressure and flowing water, the air micropockets eventually dissolve into the ambient water or burst and diminish. Herein, we analyze from first principles an air mass transfer problem. Using integral methods, we extend our prior laminar flow solution to turbulent flows. We introduce an effective slip to the turbulent boundary layer characterized by a modified 1/7-power law velocity profile. We then introduce the hydrodynamic solution to the two-dimensional problem of alternating solid–water and air–water interfaces to determine the convective mass transfer of air's dissolution into water. This situation simulates spanwise microridges, which is one of the geometries used for producing superhydrophobic surfaces. The decoupled mass-transfer problem is solvable using an approximate integral method previously optimized by Reynolds, Kays, and Kline (1958). A mass-transfer correlation is derived as a function of the surface geometry (or gas area fraction), Reynolds number, and Schmidt number. Longevity, or time-dependent hydrophobicity, could be estimated from the resulting mass-transfer correlation. As expected, turbulence greatly enhances the rate of convective mass transfer, and thus superhydrophobicity is not maintained as long as it would be under corresponding laminar flow conditions.

1. INTRODUCTION

Superhydrophobic surfaces employ optimally designed surface chemistry and roughness to repel water. They are characterized by water droplets beading on the solid surface at static contact angles (CA) exceeding 150°, and by significantly low contact-angle hysteresis. Amongst several others, examples of such surfaces in nature are the self-cleaning lotus leaves [1]. When submerged, these surfaces can entrap air between their micro- or nanostructures resulting in a surface with alternating air–water and solid–water interfaces. The presence of the air–water interface is responsible for the "slip effect", resulting in a reduction in the skin-friction drag exerted on a moving surface [2, 3]. Rothstein [2] reports drag reduction exceeding 40% and 50% in, respectively, laminar and turbulent flows, although Gad-el-Hak [4] argues that the turbulent flow results are less reliable.

Most engineered superhydrophobic surfaces are made up of microposts or microridges manufactured via advanced microfabrication techniques [5, 6]. Large-scale manufacturing of such surfaces is prohibitively expensive. An alternative solution to circumvent the high cost is to produce surfaces made up of random deposition of hydrophobic particles or electrospun fibers [3]. Along with the challenges of microfabrication, the lifetime of the surface is also a factor for the applicability of the coating. As long as air pockets are entrapped in the coating's pores, the surface remains superhydrophobic. In other words, the degree of hydrophobicity depends on the amount of air entrapped on the surface. The longevity of a superhydrophobic coating–how long the surface could maintain the entrapped air–is critical, especially in underwater applications. When the surface is subjected to flow, the longevity decreases because the flow enhances the dissolution of the entrapped air into water [7]. Once all air has escaped, the surface becomes completely wetted (Wenzel state [8]). It is expected that the longevity will decrease even more as a result of turbulence; however, there is limited literature on this subject [2, 9, 10, 11].

In this work, we develop a first-principles model using the integral method to determine the mass transfer of air from a superhydrophobic surface (i.e., longevity of the surface) subjected to turbulent flow. The roughness of the surface is assumed to be in the form of spanwise microridges. This is an expansion of our previously published laminar model [12], but with notable adjustments to accommodate the turbulent regime. A single phase flow is assumed with linearized boundary conditions. It is recognized that more accurate modeling may be achieved. However, these may not provide the same ease as that of the integral method employed herein. Next section describes our theoretical approach. This is followed by Section 3 in which the results are presented and a mass-transfer correlation is developed. Conclusions are given in Section 4.

2. THEORETICAL APPROACH

Turbulent boundary layer flow is considered over a superhydrophobic surface comprised of spanwise microridges, as shown in Figure 1. The solution is obtained for different Reynolds numbers (based on plate length), Schmidt numbers (ratio of water kinematic viscosity, v, to mass diffusivity of air into water, D), and gas area fractions (ratio of shear-free surface area to total surface area). After a relatively long starting length of 1 m, the plate is considered as alternating sections of no-slip solid–water

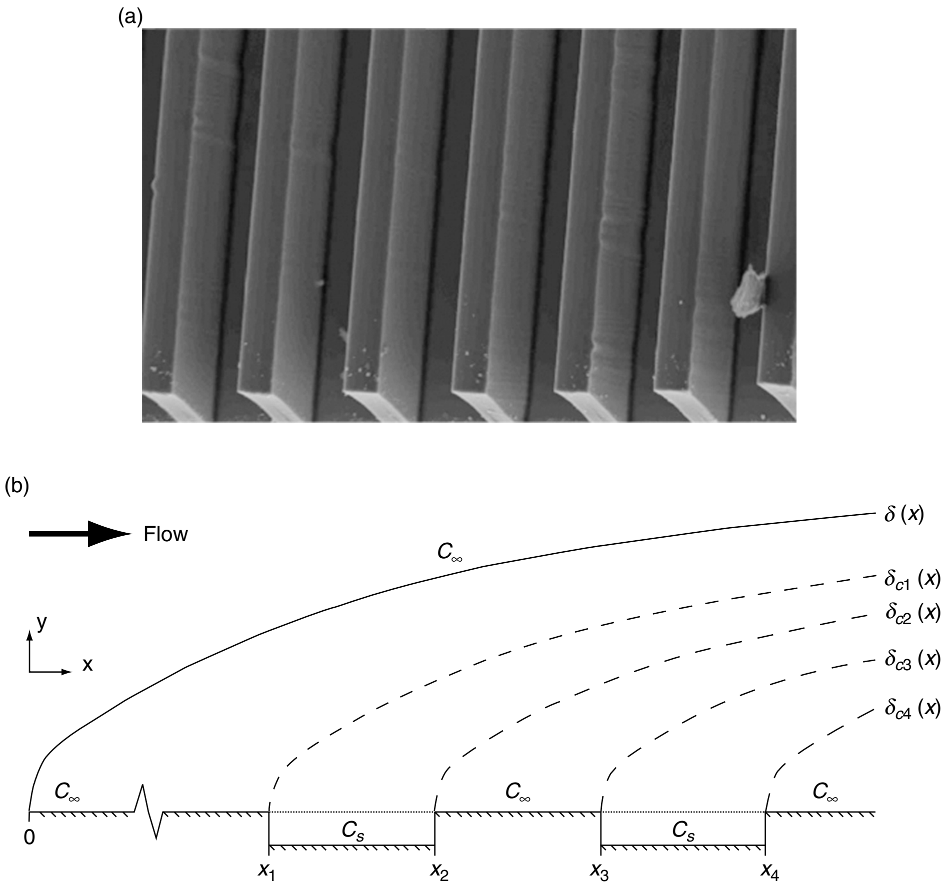

Figure 1. (a) SEM image of spanwise ridges to effect superhydrophobicity, from Maynes et al. [13]. (b) Schematic of both hydrodynamic and mass-transfer boundary layers evolving over microridges [12].

interface with zero concentration of air (same as the pure water assumed in the freestream, $C_\infty = 0$) and free-shear air–water interface with 100% saturation of air C_s. The hydrodynamic boundary layer thickness, $\delta(x)$, continuously evolves in the flow direction. At each change in position x_1, x_2, …, there is a newly growing mass-transfer boundary layer thickness, $\delta_C(x)$, due to the abrupt change in the concentration boundary condition.

As was the case in our previous paper [12], two observations are noteworthy. First, the integral relations developed are exact in the laminar case and near-exact in the turbulent flow case. However, the velocity and concentration profiles inserted into the integral relations are approximate. Solutions obtained are therefore approximate. Second, the concentration boundary condition at the solid-water interface downstream of the starting length should be, strictly speaking, $[\partial C/\partial y]_{y=0} = 0$, i.e., zero-mass-flux boundary condition. The boundary condition at the air-water interface is correct as stated above, $[C]_{y=0} = C_s$. However, the use of mixed Dirichlet and Neumann boundary conditions would preclude the employment of the superposition principle to be described in Section 2.2. The present model, though difficult to realize in practice, provides a first-principles analytical result, which is indeed rare. In the analogous heat transfer problem, alternating hot and ambient temperatures are used in order to enable the use of the superposition principle. This situation requires heated and cooled portions of the plate, which is different from heated and unheated portions.

2.1. Integral Method

The integral method is derived from the momentum and species conservation equations. The following integro-differential equations are universally accepted, for both laminar and turbulent flows [14]:

$$\frac{d}{dx}\int_0^{\delta(x)} u(y)\,(U_\infty - u(y))dy = \nu\left(\frac{du}{dy}\right)_0 \tag{1}$$

$$\frac{d}{dx}\int_0^{\delta_C(x)} \left[\frac{u(y)}{U_\infty}\right](1-\theta)\,dy = St_m \tag{2}$$

where, for turbulent flows, $u(y)$ is the mean velocity profile, U_∞ is the freestream velocity, $\delta_C(x)$ is the concentration boundary layer thickness, St_m is the Stanton mass number, and θ is the dimensionless mean concentration profile of dissolved air in water. If the species equation is to take the form written in Equation (2), it is assumed that the difference between C_{wall} and C_∞ is constant [15]. In the present formulation, this is postulated to be the case over a particular segment of the surface, i.e. solid portion or air cavity.

The integral method needs an appropriate approximation for the mean velocity and concentration profiles. For turbulent boundary layers, the widely accepted profiles are [16]:

$$\frac{u(y)}{U_\infty} = \left(\frac{y}{\delta}\right)^{1/7} \tag{3}$$

$$\theta \equiv \frac{C_{wall} - C(y)}{C_{wall} - C_\infty} = \left(\frac{y}{\delta_C}\right)^{1/7} \tag{4}$$

It is worth mentioning that the mass transfer solution is decoupled from the hydrodynamic problem, and that the concentration profile, Equation (4), is valid for different velocity profiles at different locations along the plate. Superhydrophobic surfaces generate slip flow, which could be characterized by the effective slip length S [17]. Figure 2 schematically shows the effect of slip on the velocity profile. The 1/7-power law velocity profile for no-slip condition, Equation (3), could be modified to include a slip flow.

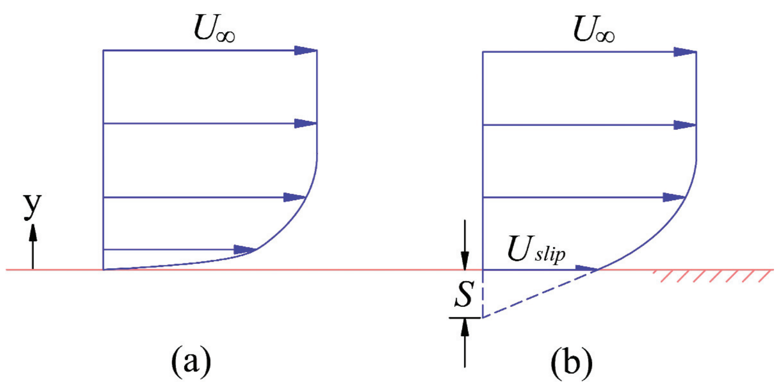

Figure 2. Schematic diagram of velocity profiles for flow over flat plate in case of (a) no slip; and (b) slip flow.

$$\frac{u(y)}{U_\infty} = \left(\frac{y+S}{\delta}\right)^{1/7} \tag{5}$$

From Equation (5) and from the figure, it is obvious that u (0) is a constant, U_{slip}, while the equation retains the one-seventh power approximation of turbulence. Solving the integral equations for a turbulent boundary layer is complicated owing to the existence of indefinite result in the derivative of the velocity and concentration profiles at the wall. In 1958, Reynolds et al. [15] proposed what is now a widely accepted solution by assuming that the momentum eddy diffusivity, ε_M, is equal to the concentration eddy diffusivity, ε_C, and that their respective diffusion mechanisms are

$$\frac{\tau_{bl}}{\rho} = \varepsilon_M \frac{\partial u}{\partial y} \tag{6}$$

$$m''_{bl} = -\varepsilon_c \frac{\partial C}{\partial y} \tag{7}$$

where $\tau_{bl}(x, y)$ is the shear stress, ρ is the density of the flowing fluid, and m''_{bl} (x, y) is the mass flux of air to dissolve in water.* Strictly speaking, the two equations above hold only far away from the wall where viscous effects are negligible and all the momentum and mass transfer are due to turbulent eddies [15]. Reynolds et al. constructed ε_M and ε_C so that the wall shear and mass flux are finite and have their correct values even at the wall. Equation (6) could be solved for ε_M utilizing the full momentum equation and tedious algebra to yield

$$\frac{\varepsilon_M}{v} = 7\frac{\delta(x)}{x}\frac{C_f}{2}\mathrm{Re}_x\left[1-\left(\frac{y}{\delta(x)}\right)^{9/7}\right]\left(\frac{y}{\delta(x)}\right)^{6/7} \tag{8}$$

The eddy diffusivity in this formulation is zero both at the wall and at the outer edge of the hydrodynamic boundary layer. Equation (1) is rewritten as

$$\frac{C_f}{2} = \frac{d}{dx}\int_0^{\delta(x)} \frac{u(y)}{U_\infty}\left(1-\frac{u(y)}{U_\infty}\right)dy \tag{9}$$

*Reynolds et al. (1958) considered a heat transfer problem. However, barring dissipation effects, the heat transfer and mass transfer problems are identical.

Similarly, Equation (7) could be solved for the Stanton mass number

$$St_m = \frac{C_f}{2}\left(\frac{\delta_C(x)}{\delta(x)}\right)^{-1/7} \tag{10}$$

where the skin friction coefficient is defined as $C_f \equiv 2\tau_{bl}\big|_{y=0}/(\rho U_\infty^2)$. The Stanton mass number can be expressed as $St_m = h_m/U_\infty$. The term h_m is the air mass transfer convection coefficient. Thus, Equation (10) could be readily solved for h_m provided that the hydrodynamic boundary layer thickness is already computed. Reynolds et al. [15] used the approximation $\delta(x) \sim x^{4/5}$. However, due to the slip nature of a superhydrophobic surface, Reynolds et al.'s approximation is not valid in our case. The original equation was formulated based largely on experimental data in turbulent pipe flow. Therefore, we assume our base equation as

$$\frac{d}{dx}\int_0^{\delta(x)} u(y)(U_\infty - u(y))dy = 0.0225U_\infty^2\left(\frac{\nu}{U_\infty\delta}\right)^{1/4} \tag{11}$$

where the right hand side is an empirical correlation. We attempted to solve for δ using Equation (5). However, for ease of calculations and because the integral analysis is an approximate method, the hydrodynamic boundary layer thickness is empirically expressed as [18]:

$$\delta = 0.37x\left(\frac{xU_\infty}{\nu}\right)^{-1/5} \tag{12}$$

2.2. Convection Coefficient

The integral method could be used to find the value of the local convection mass transfer coefficient, which could be substituted in the following equation to obtain the average coefficient along the entire plate. The superposition procedure was previously discussed by Barth et al. [12] and Bejan [14], and leads to the following equation for the total mass transfer convection coefficient

$$\bar{h}_{m_{Total}} = \mathcal{L}^{-1}\sum_{j=1}^{n}\sum_{i=1}^{j}(-1)^{i+1}\int_{x_j}^{x_{j+1}} h_i(x)dx \tag{13}$$

where n is the total number of peaks and troughs (Figure 1), $\mathcal{L}$ is the extent of the entire superhydrophobic region, and $h_i(x)$ is a local mass transfer convection coefficient.

We developed a code using Mathematica to solve the above equation for the Reynolds number range of 2×10^5–10^6. We also changed the Schmidt number according to a temperature range of 25–5°C. The change in temperature influences the dynamic viscosity μ, mass diffusivity D, and Schmidt number Sc, according to the following equations [14]:

$$D(T) = D(T_0)\frac{T}{T_0}\frac{\mu(T_0)}{T\mu(T)} \tag{14}$$

$$Sc(T) = \frac{\nu(T)}{D(T)} \tag{15}$$

where T_0 is the reference temperature value of 20°C, and T is any temperature at which both the diffusivity and Schmidt number are calculated. The resulting range of Schmidt numbers is 313–964. We ran our code for a gas area fraction (the ratio of free-shear area to the total surface area) of 50–90%.

The periodicity of the microridges of the surface (Figure 1) is fixed at 200 μm. Gas fraction increases are achieved by reducing the width of each ridge. The solution is obtained for a total of 1000 consequent sections (500 peaks and 500 troughs) following the prescribed starting length of 1 m.

2.3. Slip Length

We utilized the values of effective slip length originally found by our previously published laminar flow simulations [12]. To our knowledge, there does not presently exist more accurate data for effective slip length for turbulent flows. The closest value is that provided by Rothstein's group [9, 10]. For one particular Reynolds number, Rothstein et al. found an approximate slip length of 120 μm, with a fixed pitch of 120 μm. When our code utilized that slip length, in contrast to the one computed from full numerical simulations of the laminar boundary layer, we obtained a percentage change in the average mass flux of 42.5%.

3. RESULTS AND DISCUSSION

3.1. Effect of Surface Microstructure and Flow Properties

The above system of equations is solved numerically to show the impact of Reynolds number, Schmidt number, and gas area fraction on the rate of air dissolution into water. The dimensionless air mass transfer convection coefficient (Sherwood number) and mass flux are calculated to investigate the rate of air mass dissolution into water at the superhydrophobic surface.

Figure 3 shows the dimensionless air mass transfer convection coefficient and mass flux calculated using both the turbulent and laminar models at different Reynolds numbers. The laminar model was previously described by Barth et al. [12]. As expected both the average mass flux and Sherwood number are substantially increased in case of turbulent flow. The presence of turbulence enhances the air dissolution in water, and the mass flux is increased by one order of magnitude.

Figure 4 shows Sherwood numbers versus gas area fractions at different Reynolds and Schmidt numbers. It is obvious that as Reynolds number increases, Sherwood number increases because the

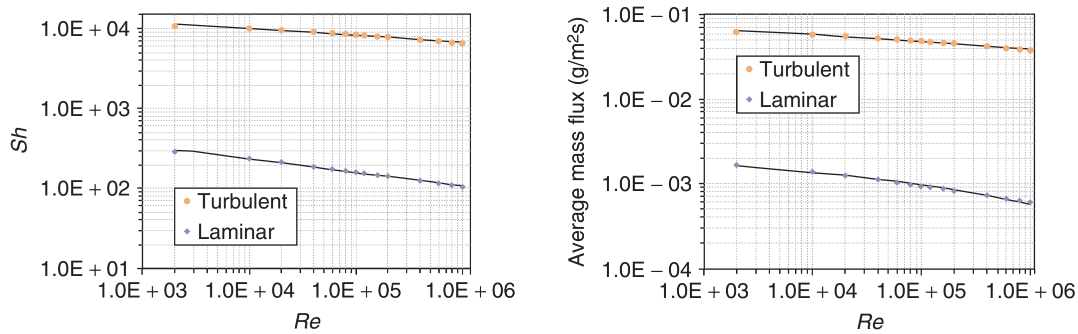

Figure 3. Comparison between Laminar [12] and turbulent models at U_∞ = 1m/s and ϕ_g = 50%. (a) Sherwood number versus Reynolds number. (b) Average air mass flux versus Reynolds number.

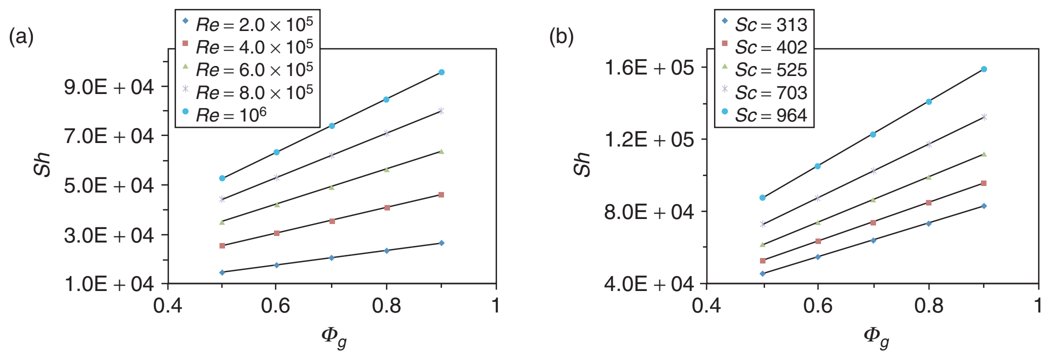

Figure 4. Sherwood number versus gas fraction. (a) At different Reynolds number with Schmidt number = 400. (b) At different Schmidt number with Reynolds number = 10^6.

flow becomes more turbulent, which leads to enhancing the dissolution of air into water. Furthermore, the increase of gas fraction increases the Sherwood number due to the enlargement of the surface area subjected to air mass transfer. Finally, the Sherwood number increases with Schmidt number. These trends qualitatively agree with both our laminar flow results [12] and the canonical no-slip case [14].

3.2. Longevity

Longevity of superhydrophobic surfaces depends on how long the surface can entrap air. Figure 5 shows the effect of Reynolds and Schmidt numbers and the impact of gas area fraction on the rate of air dissolution into water. It is obvious that the mass flux is enhanced by increasing the gas area fraction and Reynolds number. However, the mass transfer decreases with Schmidt number owing to the reduction in the mass diffusivity of air into water, D. This agrees qualitatively with the results reported for the laminar studies [7, 12]. Mass transfer is directly related to the lifetime of a superhydrophobic surface, or surface longevity. Higher mass flux indicates an acceleration of air dissolution into water, i.e., reduced longevity.

3.3. Mass-Transfer Correlation

We propose a correlation to express the Sherwood number as a function of Reynolds number (flow property), Schmidt numbers (fluid property), and gas area fraction (surface morphology) in the form

$$Sh_x = f\left(\mathrm{Re}, Sc, \phi_g\right) \tag{16}$$

The well known classical correlation for mass-transfer forced convection from a solid flat plate (with no-slip condition; $\phi_g \to 0$) subjected to a turbulent flow reads.

$$Sh_x = 0.0296\,\mathrm{Re}^{4/5}\,Sc^{1/3} \tag{17}$$

As $\phi_g \to 1$, there is near perfect slip, and the hydrodynamic boundary layer is very small compared to the concentration boundary layer. In that case, $u(y) \approx U_\infty$, and the differential mass transfer equation could readily be integrated. The solution is

$$Sh_x = \frac{1}{\sqrt{\pi}}\mathrm{Re}_x^{4/5}\,Sc^{1/2} \tag{18}$$

The following correlation is proposed for slip flow. The formula is similar to that presented in our laminar studies [12], but with a modified exponent of the Reynolds number to accommodate the effect of turbulence

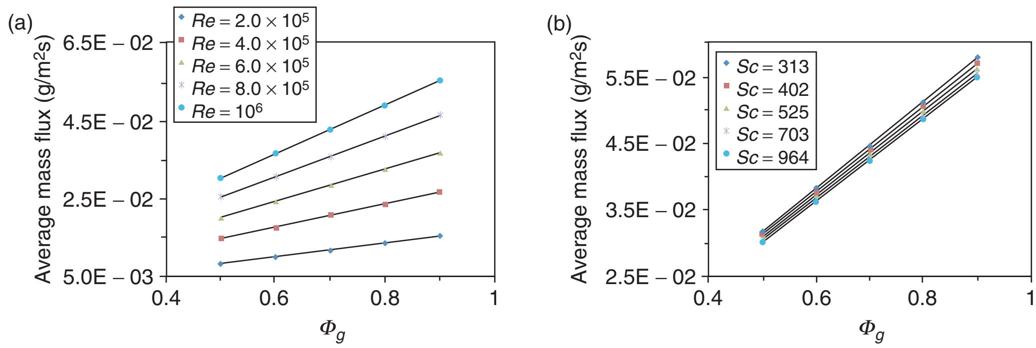

Figure 5. Average air mass flux versus gas fraction. (a) At different Reynolds number with Schmidt number = 400. (b) At different Schmidt number with Reynolds number = 10^6.

$$Sh = K\phi_g \,\mathrm{Re}^{4/5}\, Sc^{\left(\frac{1}{3}+\frac{\phi_g}{6}\right)} \tag{19}$$

where Sh is the Sherwood number averaged over the superhydrophobic region. In the above correlation, if we allow the gas area fraction to approach $\phi_g = 0$ and $\phi_g = 1$ (the two extremes of gas area fraction), the Schmidt number exponent becomes, respectively, 1/3 and 1/2, which agrees with the canonical cases of respectively no slip and perfect slip. Regression analysis of the data presented in Figure 4 yields $K = 0.1083$. This value is not too different from $K = 0.145$ computed for the laminar case [12]. Of course the different Reynolds number exponents in the laminar and turbulent cases greatly affect the respective values of the Sherwood number.

4. CONCLUSIONS

In this work, a first-principles model was developed to predict the rate of convective mass transfer of air from superhydrophobic surfaces subjected to turbulent flow. The proposed integral method is approximate; however, it does not require the computer-intensive calculations demanded by direct numerical simulations. The mass transfer problem was solved using the integral method, and a mass-transfer correlation was developed. The estimated rate of mass transfer reflects how long the surface can keep its hydrophobicity, i.e., longevity. While turbulent flow over superhydrophobic surfaces promise to increase drag reduction by about 20% more than that of laminar flow, the longevity is found to decrease by one order of magnitude. This work could be extended to include different boundary conditions and more accurate approximations for the hydrodynamic boundary layers and effective slip length.

ACKNOWLEDGMENTS

This research is sponsored by the Defense Advanced Research Projects Agency (DARPA), contract numbers W91CRB-10-1-0003 and W911QX-12-1-0001, technical sponsor Captain Christopher Warren, USN. The content of this paper does not necessarily reflect the position or the policy of the United States Government, and no official endorsement should be inferred.

REFERENCES

[1] Neinhuis, C., Barthlott, W., Characterization and distribution of water-repellent, self-cleaning plant surfaces, *Ann. Bot.*, 1997, 79(6), 667–677.

[2] Rothstein, J. P., Slip on superhydrophobic surfaces, *Annu. Rev. Fluid Mech.*, 2010, 42, 89–109.

[3] Samaha, M. A., Tafreshi, H. V., Gad-el-Hak, M., Superhydrophobic surfaces: From the lotus leaf to the submarine, *C. R. Mec.*, 2012, 340(1), 18–34.

[4] Gad-el-Hak, M., Comment on "Experimental study of skin friction drag reduction on superhydrophobic flat plates in high Reynolds number boundary layer flow", *Phys. Fluids*, 2013, 25, 079101.

[5] Ou, J., Perot, J. B., Rothstein, J. P., Laminar drag reduction in microchannels using ultrahydrophobic surfaces, *Phys. Fluids*, 2004, 16, 4635–4643.

[6] Lee, C., Choi, C-H., Kim, C-J., Structured surfaces for giant liquid slip, *Phys. Rev. Lett.*, 2008, 101(6), 064501.

[7] Samaha, M. A., Tafreshi, H. V., Gad-el-Hak, M., Influence of flow on longevity of superhydrophobic coatings, *Langmuir*, 2012, 28(25), 9759–9766.

[8] Wenzel, R. N., Resistance of solid surfaces to wetting by water, *Ind. Eng. Chem.*, 1936, 28(8), 988–994.

[9] Daniello, R. J., Waterhouse, N. E., Rothstein, J. P., Drag reduction in turbulent flows over superhydrophobic surfaces, *Phys. Fluids*, 2009, 21, 085103.

[10] Martell, M. B., Perot, J. B., Rothstein, J. P., Direct numerical simulations of turbulent flows over superhydrophobic surfaces, *J. Fluid Mech.*, 2009, 620, 31–41.

[11] Woolford, B., Prince, J., Maynes, D., Webb, B. W., Particle image velocimetry characterization of turbulent channel flow with rib patterned superhydrophobic walls, *Phys. Fluids*, 2009, 21, 085106.

[12] Barth, C. A., Samaha, M. A., Tafreshi, H. V., Gad-el-Hak, M., Convective mass transfer from submerged superhydrophobic surfaces, *Int. J. Flow Control*, 2013, 5, 79–88.

[13] Maynes, D., Jeffs, K., Woolford, B., Webb, B. W., Laminar flow in a microchannel with hydrophobic surface patterned microribs oriented parallel to the flow direction, *Phys. Fluids*, 2007, 19, 093603.

[14] Bejan, A., *Convection Heat Transfer*, 3rd edn., John Wiley & Sons, Hoboken, New Jersey, USA, 2004.

[15] Reynolds, W. C., Kays, W.M., Kline, S. J., Heat transfer in the turbulent incompressible boundary layer. II- Step wall-temperature distribution, NASA Memorandum 12-2-58W, Washington, DC, 1958.

[16] Kays, W.M., Crawford M. E., *Convective Heat and Mass Transfer*, 3th edn., McGraw-Hill, New York, USA, 1993.

[17] Navier, C. L. M. H., Memoire sur les lois du mouvement des fluides, *Mem. Acad. R. Sci. Inst. France*, 1893, 6, 389–440.

[18] Schlichting, H., *Boundary-Layer Theory*, 7th edn., McGraw-Hill, New York, USA, 1979.